Theoretical Study of Electron Transfer in Ferrocytochromes

A. A. Stuchebrukhov† and R. A. Marcus*,‡

Department of Chemistry, University of California, Davis, California 95616, and Arthur Amos Noyes Laboratory of Chemical Physics, 127-72, California Institute of Technology,§ Pasadena, California 91125

Received: September 22, 1994; In Final Form: December 28, 19948

A series of calculations is reported of the superexchange electronic matrix element between donor and acceptor states in photoinduced long-distance electron-transfer reactions in seven Ru-modified proteins: Ru(bpy)2im-(HisX)-cyt c, where X = 33, 39, 58, 62, 66, 72, 79. Calculated results are compared with experimental data. The model used for the calculation includes a detailed description of the donor and acceptor wave functions in terms of ligand field theory. The intervening protein medium is treated within the extended Hückel theory. It is found that the symmetry and spatial properties of the donor/acceptor wave functions impose certain selection rules on the pathways used in electron transfer. Some paths through σ bonds are not allowed due to the symmetry requirement, for example. Also, the influence of the spatial mutual orientation of the donor and acceptor orbitals in the protein on the rates of electron transfer is analyzed. It is found that there is a strong stereochemical effect in this type of reaction. The mutual orientation of the orbitals is an important factor which determines the reaction rate, in addition to such factors as distance between donor and acceptor and concrete chemical structure of the protein matrix discussed before in the literature. In the calculations, a new method of transition amplitudes is applied. The method can be used for proteins and other large systems involving several thousand atoms. Numerically, the new method reduces the calculation of the electronic coupling between donor and acceptor to the problem of finding iteratively the minimum of a multidimensional parabola, and avoids the diagonalization of the Hamiltonian matrix.

I. Introduction

Long-distance electron transfer plays a central part in many biological processes, such as photosynthesis and respiration.¹ It is believed, also, that the long-distance charge separation will be used in future artificial photosynthetic systems² and in molecular electronic devices,³ mimicking the natural processes. Much effort has therefore been directed in the past toward understanding this type of electron-transfer reaction. Recent elucidation of the crystallographic structure of many natural electron-transfer systems, in particular those of photosynthetic reaction center⁴ and several electron-transfer proteins, has advanced research in this field on a molecular level so that a detailed comparison between theoretical calculations and experimental data is now possible.

In this paper, we report on a series of calculations of the superexchange matrix element between donor and acceptor states in seven electron-transfer ferroproteins: Fe(heme)-cyt- $Ru(HisX)(bpy)_2im$, where X = 79, 72, 66, 62, 58, 39, 33. The results are compared with recent experimental data. Electron transfer occurs in these systems between Fe2+/3+ and Ru3+/2+ ions. The Ru complex is coordinated to the surface HisX amino acid, and the Fe ion is located in the heme porphyrin ring inside the protein. The distance between donor (Fe2+) and acceptor (Ru³⁺) varies in the range 13-20 Å. The protein matrix separating donor and acceptor provides a medium which facilitates (in fact, makes possible) electron transfer over such long distances.^{5,6} These electron-transfer systems were designed and synthesized by Gray and co-workers, 7-9 and experimental data on the electron-transfer rates were published recently.^{7,8} The data files with crystallographic structures of these compounds for the present studies were kindly provided to us by Jay Winkler.

In the experimental studies, a very fruitful idea has been used to choose a Ru–acceptor complex so as to compensate the reorganization energy of the reaction by the driving force. As a result, electron transfer in these systems is almost activationless. 10,11 Comparison between experimental rates and theoretical calculations in such systems then involves the minimum uncertainty in the effect of parameters such as ΔG^0 of the redox pair. Several fundamental questions on the distance dependence and on the role of the protein structure in electron-transfer processes in natural biological systems can be addressed in these studies. A detailed review of the experimental work and discussion has been given in the literature. 5,6

Theoretical calculation of the reaction rates in systems involving thousands of atoms at a detailed molecular level presents an enormous challenge, even when the structure of these systems is known. Recently, several such theoretical studies have been reported in which dynamical^{12–14} and electronic coupling aspects^{15–29} of biological electron-transfer reactions were addressed. In particular, the superexchange matrix element was calculated by several groups^{17–29} for systems similar to those considered in the present study. The problem is usually treated in a one-electron approximation (for an exception, see ref 16), and due to recent advances in Green's function technique,^{24–29} all atoms of the system can be included in the calculation. In this paper, the theory is advanced in several major aspects, compared with the previous work.

Most importantly, in the present paper the donor and acceptor wave functions are given a detailed consideration. The wave functions are constructed from the five d orbitals of the transition-metal ions with the use of ligand field theory concepts³⁰ and of spectroscopic experimental data on the metal complexes involved in the reaction.^{31,32} We find that the symmetry of the donor and acceptor states, defined by the

[†] University of California.

[‡] California Institute of Technology.

[§] Contribution No. 8990.

^{*} Abstract published in Advance ACS Abstracts, May 1, 1995.

symmetry of the ligand fields in the heme and in the Ru complex, is crucial in the relative importance of tunneling paths 17 through a network of σ or π molecular orbitals connecting donor and acceptor states. Thus, the symmetry of the donor—acceptor states imposes selection rules on the tunneling paths, and certain tunneling paths connecting donor and acceptor are not allowed. It is shown that the correct symmetry of the donor—acceptor wave functions provides a strong coupling to a π orbital system of the intervening protein matrix. Some preliminary comparison with the method of extended amino acid pathways 21,22 is also given. We find that the concept of amino acid pathways provides a reasonable reduction of the total protein. The conclusion is based on the comparison of the all-atom calculations and the reduced model of the protein.

Computationally, a new method of transition amplitudes introduced in ref 29 by one of us, an alternative to evaluating Green's functions, is used for the nonperturbative calculation of the matrix element. All atoms of the system (approximately 1800 atoms and 4500 orbitals) are included in the calculation which takes less than 30 s of CPU time on a CRAY computer. Numerically, the problem is reduced to finding a minimum of multidimensional parabola. A conjugate gradient method is used to solve this problem. The method takes full advantage of the sparsity of the Hamiltonian matrix and can be applied in the future to systems involving hundreds of thousands of orbitals.

The problem of overlapping orbitals (nonorthogonal basis set) is addressed in our calculations. Also, we consider the problem of electron transfer between several degenerate or near-degenerate states of the donor and acceptor, which arises in the case in the reaction involving two transition-metal complexes.

The paper is structured as follows. In section II, basis sets, a model Hamiltonian, and the method of transition amplitudes are reviewed. In the next section, III, the donor—acceptor wave functions are analyzed and the implications of the symmetry properties of these functions for the superexchange coupling are discussed. In section IV, results of calculations and comparison with experimental data are presented.

II. Superexchange Coupling and the Method of Transition Amplitudes

The present theory is an effective one-electron picture, where the antisymmetric properties of multielectronic wave functions are included only via the Pauli principle. The matrix element $H_{DA}(E)$ between the donor state D and the acceptor state A is given by the well-known expression^{21–29}

$$H_{\mathrm{DA}}(\mathrm{E}) = \sum_{\alpha} \frac{V_{\mathrm{A}\alpha} V_{\alpha \mathrm{D}}}{(E - E_{\alpha}^{\mathrm{B}})} = \sum_{\alpha} \langle A | V | \alpha \rangle \frac{1}{(E - E_{\alpha}^{\mathrm{B}})} \langle \alpha | V | D \rangle$$
(2.1)

where $H^{\rm B}$ is the Hamiltonian of the bridge, V is the coupling between bridge orbitals and donor and acceptor orbitals, and E is the tunneling energy (energy of the donor and acceptor orbitals at the transition state). The states $|\alpha\rangle$ denote the eigenstates of the bridge Hamiltonian $H^{\rm B}$ and $E^{\rm B}_{\alpha}$ its eigenvalues. The direct (nonbridge mediated) coupling $\langle A|V|D\rangle$ is omitted in eq 2.1.

It is usually assumed that there are no resonances between states in the bridge and the donor—acceptor states and that all the states $|\alpha\rangle$ with energies below E in eq 2.1 are doubly occupied and those above E are unoccupied. The contribution of the occupied energy levels of the bridge can be associated with the hole transfer and contribution of unoccupied levels with

electron transfer. Both the hole-transfer and electron-transfer contributions are present in the total matrix element (2.1).

The above equation is obtained from the more general $expression^{24-29}$

$$H_{DA}(E) = \langle A | V(E - H^{B})^{-1} V | D \rangle \tag{2.2}$$

by inserting on both sides of the resolvent operator $(E-H^{\rm B})^{-1}$ the expansion of unity in terms of the orthogonal and complete basis set of eigenstates $|\alpha\rangle$ of the bridge Hamiltonian $H^{\rm B}$. Equation 2.2 is the lowest order expression in the strength of coupling to the bridge, V. As will be argued in the next section, this approximation is sufficient for description of electron transfer in the present case, namely, between low-spin transition-metal complexes with less than six electrons in the d shell. In a more general case of arbitrary coupling V, the qualitative picture remains the same.

Thus, if one could diagonalize the bridge Hamiltonian H^B , then the above expression could be computed using eigenstates and eigenvectors of H^B and using eq 2.1. Such a procedure has been used in refs 19–22 for a reduced model of a protein, namely, where only the physically most important chemical units were considered, as determined by an artificial intelligence search procedure using an evaluation function. In that case, a direct diagonalization was readily performed.

Alternatively to eq 2.1, one can calculate expression 2.2 with any other suitable basis set $|i\rangle$ for the bridge. In the present paper, for example, the extended Hückel basis set³³ is used. Other basis sets are also possible. For a nonorthogonal basis set (a basis with overlaps), as for the present case of the extended Hückel basis, the matrix element expression takes the form (details are given in the Appendix)

$$H_{\mathrm{DA}}(E) = \sum_{i,j} \langle A|V|i\rangle (ES - H^{\mathrm{B}})_{ij}^{-1} \langle j|V|D\rangle \qquad (2.3)$$

where S is the overlap matrix, $S_{ij} = \langle i|j\rangle$, and H^B is the Hamiltonian marix of the bridge in the basis $|i\rangle$. This expression is different from the one recently published in refs 27 and 28. To our knowledge, the nonorthogonality problem was not addressed in other studies on this subject.

This second method of calculation given by eq 2.3 does not require the diagonalization of the matrix H^B , but it does require, at first glance, the inversion of the matrix $ES - H^B$. Since the inverse of this matrix is Green's function of the bridge, that method is known as Green's function method. A number of numerical procedures for direct inversion of the Hamiltonian matrix have been discussed in the literature. The effectiveness of this method for a large system involving of the order of 10 000 orbitals or larger depends upon the availability of the efficient computer inversion routines for sparse systems.

In this paper, we use, instead, another method, which is equivalent to Green's function method in the sense that it gives an exact nonperturbative solution to the problem of evaluating (2.3). However, the calculation is performed in a different way, which does not require the inversion procedure. Instead of the inversion, the sparse system of linear equations is solved for the transition amplitudes defined below. For sparse linear systems, there are many iterative methods available. The use of an appropriate iterative method can yield an approximate solution significantly faster than the direct method. Also, iterative methods require less memory than the direct methods, making iterative methods the only feasible approach for very large systems.^{34,35}

In the transition amplitudes method,²⁹ the matrix element is written as

$$H_{\mathrm{DA}}(E) = \sum_{i} A_{i}^{+} T_{i} \tag{2.4}$$

where the vector $A_i^+ = \langle A|V|i\rangle$ and the T_i 's are the transition amplitudes. The T_i 's describe the amplitudes of superexchange transitions between the donor orbital $|D\rangle$ and the orbitals $|i\rangle$ in the bridge. For the transition amplitudes T_i , one has a system of linear equations

$$D_i = \sum_j (ES - H^{\rm B})_{ij} T_j \tag{2.5}$$

where the vector $D_i = \langle i|V|D\rangle$. Thus, instead of inverting the matrix $ES - H^B$ and calculating Green's function of the bridge, one can solve a system of linear equations (2.5) for the transition amplitudes T_i . This last problem for sparse systems is reduced to the equivalent numerical problem of finding a minimum of a multidimensional parabola (the condition for minimum is given by eq 2.5), and then the problem is solved by the conjugate gradient method.^{36,37} This method allows one to treat extremely large systems with hundreds of thousands of linear equations.³⁵

Such a method has been implemented by us on a Cray computer in conjunction with a graphics input interface program BIOGRAF.³⁸ The calculation by this method of the total matrix element in Ru-modified cytochrome c from experiments of Gray and co-workers, involving an all-atom model of the protein (about 1800 atoms and 4500 orbitals), takes less than 30 s of one CRAY Y-MP CPU time.

The advantage provided by the method of transition amplitudes, compared with the exact diagonalization procedure (2.2), is balanced by the lack of detailed information about the contributions of the individual energy levels in $H_{DA}(E)$. Also, the contributions of the hole transfer and electron transfer are given now only as a sum in the total matrix element $H_{DA}(E)$. It is sometimes useful to know these contributions separately. A method which allows a separation of the contribution of the hole transfer from that of the electron transfer without the diagonalization procedure is described in ref 29.

III. Donor and Acceptor Wave Functions

Ligand field theory provides an appropriate description of the one-electron wave functions for donor and acceptor states. In much of our discussion, we follow a standard text on this subject³⁰ and use experimental spectroscopic data from ref 31 and a recent paper of Gadsby and Thomson on the spectroscopy of hemoproteins.³²

In the reaction of present interest, $Fe^{2+/3+}$ (heme)-cyt-(HisX)- $Ru^{3+/2+}$, the transferring electron in the initial state and the final state occupies the 3d shell of Fe ion and the 4d shell of Ru, respectively. The 5-fold degenerate shells of the metallic ions are split by the low symmetry field of the six ligands coordinated to the ions in the compound. The Ru ion is coordinated by six nitrogens, including one nitrogen of the HisX residue on the surface of the protein, and the Fe ion is coordinated by the four pyrrole nitrogens of the porphyrin ring, by a nitrogen of the His18 residue at an axial position, and by the sulfur of the Met80 residue at the other axial position. In our discussion of the orbitals of the metal ions, we introduce coordinate systems for each of the metal complexes with the z coordinate directed toward the Met80 residue for Fe and toward HisX for the Ru complex.

We first consider the case when all six ligands are treated as being equivalent. The five d orbitals of the ions are then split

TABLE 1: Energies of t2g Orbitalsa

HisX, X	Fe: E_{zx} , E_{zy} , E_{xy}	Ru: E_{zx} , E_{zy} , E_{xy}
39	-10.41 - 10.46 - 10.52	-10.93 -11.12 -11.23
33	-10.46 - 10.62 - 10.68	-10.90 - 11.12 - 11.25
66	-10.46 - 10.62 - 10.68	-10.90 - 11.12 - 11.25
72	-10.46 - 10.62 - 10.68	-10.93 - 11.10 - 11.20
59	-10.41 - 10.46 - 10.50	-11.20 - 11.39 - 11.56
62	-10.41 - 10.46 - 10.52	-11.20 - 11.23 - 11.36

^a In eV. The notation for orbitals is the same as in ref 32.

into two subshells, the doubly degenerate e_g set formed by d_{z^2} and $d_{x^2-y^2}$ orbitals and a triply degenerate set t_{2g} , consisting of d_{xy} , d_{xz} , and d_{yz} . The orbitals of the e_g set are oriented toward the ligands and participate in σ bonding. Due to the interaction with the bonding orbitals of the ligands, these orbitals are mixed strongly with the ligand orbitals, and the appropriate bonding and antibonding states are pushed several electronvolts below and above the t2g subshell. In fact, most of the amplitude of the d_{z^2} and $d_{x^2-y^2}$ orbitals is concentrated in the antibonding state, which then roughly speaking coincides with the eg doubly degenerate state. The orbitals of the t2g subshell, on the other hand, interact and mix very little with the ligand orbitals because their electronic density is concentrated in between the ligands. In the low-spin systems, as in the present case, all electrons of the ions with six d electrons or less occupy the t_{2g} subshell. Six electrons of d⁶ (Fe²⁺, Ru²⁺) completely fill the t_{2g} subshell, whereas in a state with the configuration d⁵ (Fe³⁺, Ru³⁺), there is a hole in the t_{2g} subshell, and the state is a Kramers doublet.

Thus, the tunneling electron in the initial and final states is localized on the t_{2g} subshells of the metal ions. The orbitals of this subshell can be treated in the zeroth approximation as decoupled from the rest of the system. The small interaction which exists between the complexes and the bridge can then be accurately described as a first-order approximation, as we have done in the previous section.

Due to the near-octahedral symmetry of the complexes, the orbitals d_{xy} , d_{xz} , d_{yz} of the t_{2g} subshell interact mainly with the p orbitals of the ligands which are perpendicular to the ligandmetal bonds or with the orbitals of similar symmetry (e.g., with π orbitals). Hence, the superexchange electron transfer from these orbitals can be mainly mediated by the network of protein orbitals in which π orbitals of the ligands participate strongly. It is clear from this consideration that some pathways in the complex network of overlapping orbitals will not participate much in the electron transfer due to the symmetry of the donor—acceptor states. For example, the networks which start as a σ path will not participate much in the superexchange coupling under this consideration. Thus, the symmetry significantly modifies the overall picture of pathways.

The distortion of the octahedral symmetry (nonequivalence of the six ligands) will split the t_{2g} orbitals, so that the degeneracy will be completely removed. However, this additional splitting is much smaller than the octahedral splitting between t and e subshells. Experimental data^{31,32} and our molecular orbital calculations indicate that the octahedral distortion splitting is in the range of a tenth of an electronvolt or less, as seen in Table 1. In the first approximation, d_{xy} , d_{xz} and d_{yz} orbitals of the t subshell are not mixed with each other by this additional low symmetry field, and the energies of these orbitals are only slightly different from each other.

An important point is that these orbitals are "frozen" in the space with respect to the structure of the donor/acceptor complex. The electron density is localized between ligands (so that the overlap is not significant) and the symmetry of these orbitals is such that only π systems of the ligands can be effectively reached. It is between these orbitals of the donor

and acceptor electron transfer occurs. Because of the small splittings, any of these orbitals can participate in electron transfer (i.e., any of the six electrons of Fe^{2+} can be transferred to Ru^{3+} or the hole in the Ru^{3+} ion can be transferred to any of the three doubly occupied orbitals of the t_{2g} shell of the Fe^{2+} ion). Due to differences of the orbital energy, the reaction rates calculated for the individual levels will have slightly different driving forces. On the other hand, due to a rigid spatial orientation of individual orbitals of the triplet, the matrix elements for these components can differ significantly, as seen in the next section.

The theory taking into account the difference in driving force for different components of the t shell will be discussed elsewhere. In the present calculation, we note that when (as in the experiments of Gray and co-workers) the rate is near the maximum in the rate vs the driving force plot, the rate is relatively insensitive to the possible corrections to the driving force ΔG^0 in electron transfer into or from the different orbitals. Hence, in the zeroth approximation, this difference in the driving force for different components of the electron-transfer reaction can be neglected. We note, though, that it is only a rough approximation and the refinement of the theory will be made in the future

In a usual theory of nondegenerate donor and acceptor states, ^{10,11} the rate constant at the maximum in the plot rate vs driving force is given by

$$k^{\text{max}} = \frac{2\pi}{\hbar} \frac{|H_{\text{DA}}|^2}{(4\pi\lambda kT)^{1/2}}$$
 (3.1)

where λ is the reorganization energy. In the comparison of eq 3.1 for k^{max} with experimental data, it is assumed that the rate-determining step is the electron transfer, rather than some prior protein conformational change from an inactive to an active form. For a very fast electron transfer, it is possible that such a step would become rate limiting. We neglect this possibility here, in the absence of further information.

The above expression is classical but is close to the corresponding quantum expression (e.g., ref 10). The modifications of that theory due to the presence of several donoracceptor states are as follows. In the initial state, the three sublevels of the t_{2g} shell of the Fe²⁺ ion are completely filled (configuration d⁶) and there is one hole in the Ru³⁺ t_{2g} shell (configuration d⁵). In the final state, the hole occupies one of the t_{2g} levels of the Fe³⁺ ion. It is convenient, then, to think about the hole exchange between Fe and Ru ions. (This hole exchange is introduced only for the sake of description and is different from the usual hole transfer. The usual electrontransfer and hole-transfer contributions are both given by the total matrix element of our calculations.) From each of the three possible states of Ru3+, the hole can be transferred to each of the three sublevels of Fe²⁺, yielding three different Fe³⁺ states. For a given initial state of the hole in Ru³⁺, each of the charnels of the reaction (i.e., hole transfer into each of the three levels of Fe²⁺) will have a different ΔG^0 . Since the energy difference in the position of t2g levels of Fe is much smaller than the average experimental value of ΔG^0 , we can neglect the difference in energies of the final states of Fe. In this case, the total rate from each of the sublevels $|j\rangle$ of Ru will be given by a sum of rates of hole transfer into all three sublevels of Fe²⁺. The nonadiabatic rate is proportional to the square of the matrix element, as in eq 3.1. Hence, neglecting the difference in driving force, the total rate from the jth hole state of Ru³⁺ is proportional to the sum of squared matrix elements. The

effective matrix element is then a square root of a sum:

$$k_{j} \propto |H_{\mathrm{DA}}^{j}|^{2} \tag{3.2}$$

$$|H_{\mathrm{DA}}^{j}| = (\sum_{i=1}^{3} |H_{\mathrm{DA}}^{ij}|^{2})^{1/2}$$
 (3.3)

where the sum is over the three t_{2g} states of Fe.

If several Ru³⁺ states can participate in the reaction, then the contribution of each of the levels will be weighted with an appropriate Boltzmann factor and the total rate will be given by

$$k = \sum k_j p_j \tag{3.4}$$

where the p_j 's are the Boltzmann populations of the Ru t_{2g} states. The effective matrix element is then

$$|H_{\rm DA}| = (\sum_{ij=1}^{3} |H_{\rm DA}^{ij}|^2 p_j)^{1/2}$$
 (3.5)

In the case of almost degenerate states, the population of the acceptor states will be the same, and the matrix element then takes the form

$$|H_{\rm DA}| = (\sum_{i=1}^{3} |H_{\rm DA}^{ij}|^2/3)^{1/2}$$
 (3.6)

To use eq 3.5 instead of eq 3.6 one would need to know the Boltzmann factors p_j . At present, such experimental information on the Ru³⁺ t_{2g} states is not available. For this reason, we collected the calculated data for several possibilities in order to compare the various combinations with the experimental numbers. Various calculated splittings of the t subshells are given in Table 1. It would be useful to compare these data with experimental data on metal-to-ligand charge-transfer spectra in Fe²⁺ and Ru²⁺ complexes in the modified cytochrome c system.

In the calculation, the appropriate linear combinations of five d orbitals for Fe and Ru complexes were found by diagonalizing the Hamiltonian matrix formed with the extended Hückel basis set for a central metal ion and six ligands positioned according to the geometry of the complex in the protein. Although, in general, the Hückel method gives poor results for the transitionmetal complexes, we used the diagonalization only in order to find an appropriate linear combination for orbitals of the t shell, which is defined by the symmetry of the complex. Then, the energy of the appropriate orbital in the heme was assigned a value corresponding to the experimental data on charge-transfer spectra in ferric hemoproteins. The observed charge-transfer spectrum³² is due to the transition from the highest occupied π orbital of the porphyrin ring to the highest unoccupied orbital of the t_{2g} shell on the ferric ion. The procedure of adjustment of the donor state relative the highest occupied orbital of the heme according to experimental data was the same as in the previously published papers of Siddarth and Marcus. 21,22 The acceptor state was given the same energy since the transition state occurs at the intersection of the zeroth-order potential surfaces for the two electronic states D-B-A, D+-B-A- of the entire system. Again, since there is no absolute certainty in the data for the energy of the tunneling electron, we have performed calculations for different energies in the region

TABLE 2: Contribution of Individual Components of the t_{2g} Subshell to the Total Matrix Element^a

HisX,	$3(t_{2g})Ru^b$		$1(t_{2g})\mathbf{R}\mathbf{u}^c$		expt ^d	Ru-to-Fe		
	$\overline{H}_{\mathrm{DA}}^{\mathrm{xy}}$	$\bar{H}^{zx}_{\mathrm{DA}}$	$\overline{H}_{\mathrm{DA}}^{\mathrm{zy}}$	$H_{\mathrm{DA}}^{\mathrm{xy,zx}}$	$H_{\mathrm{DA}}^{\mathrm{zy,zx}}$	$H_{\mathrm{DA}}^{\mathrm{zx,zx}}$	H_{DA}	$d,^d$ Å
39	0.20	0.40	0.67	0.25	0.48	0.80	0.11	20.3
33	0.15	0.70	0.74	0.24	1.14	1.22	0.097	17.9
66	0.14	0.83	1.40	0.20	1.20	2.12	0.060	18.9
72	0.30	0.18	0.18	0.47	0.21	0.33	0.057	13.8
58	0.008	0.07	0.12	0.006	0.01	0.01	0.014	20.2
62	0.006	0.07	0.13	0.01	0.10	0.22	0.0059	20.2

 a In cm⁻¹. Matrix elements were calculated for tunneling energy $E_{\text{tun}} = -10.75 \text{ eV}$. All three levels of the Ru t_{2g} subshell are assumed to contribute equally, as in eq 3.6. The xy, zx, and zy superscripts on \tilde{H}_{DA} are for the different orbitals on Fe, xy being the lowest Fe. In a calculation based on eq 3.5 instead of eq 3.6, the Boltzmann factors p_j would be introduced. Only the upper level of the Ru t_{2g} subshell, d_{zx} , is assumed to participate in the coupling. Reference 7. The distance shown corresponds to the distance between the two metal atoms.

corresponding to the experimental data and analyzed the sensitivity of the results to these variations.

IV. Results and Discussion

In this section, the results of our calculation, performed as described in the previous sections, are presented for seven Rumodified cytochrome c compounds $Ru^{3+/2+}(bpy)_2im(HisX)$ -cyt-(heme)Fe^{2+/3+}, where X = 79, 72, 66, 62, 58, 39, 33. A Ru complex (the electron acceptor in the reaction) is coordinated to the surface of the protein at various histidines incidated by X, and the iron ion in the heme (the electron donor) is located inside the protein molecule.

These compounds were synthesized and the reaction rates were measured by Gray and co-workers. The measurements were performed with a flash-quench technique, in which the reduced ferrocytochromes were excited with a laser pulse in the absorption band of the Ru²⁺ complex; the excited electron (4d) then was quickly removed from the complex by a strong electron acceptor (Ru³⁺(NH₃)₆) from the solution, leaving a hole in the t_{2g} shell of the Ru³⁺ ion. The subsequent electron transfer from Fe²⁺ to Ru³⁺ was then measured with the transient absorption technique. The structures of these compounds were also modeled by the same group using the computer graphics and modeling program BIOGRAF. The data files for the structures were then used in our calculations.

The reorganization energy λ has been estimated to be around 0.8 eV, and the free energy of the reaction has been measured to be -0.74 eV. Thus, the reaction is almost activationless and the reaction rate, as a function of the driving force, is in the region of its maximum value.^{7,8} Using these data (and assuming that λ is the same for all compounds), together with the classical Golden Rule expression for the nonadiabatic reaction rate and the measured reaction rates, Gray and co-workers calculated the electronic coupling matrix elements corresponding to their measurements. The experimental values of these matrix elements are given in Table 2.

The distance between donor and acceptor metal ions in these compounds depends on the position of the Ru complex on the surface of the protein and varies in the range of 13.8 Å for His72 to 20.3 Å in the His39 compound.⁷ When both the reorganization energy and the driving force are the same for each compound, the variations in rate in different compounds (by some 2 orders of magnitude) reflect the changes of the square of the matrix element coupling donor and acceptor states.

In the simplest picture of the protein matrix separating donor and acceptor as a uniform medium, the electronic coupling (and the probability for electronic tunneling) should decrease approximately exponentially with distance.³⁹ According to an analysis of the group of Dutton and co-workers,⁶ the data for a variety of proteins involving rates k^{max} which vary by some 13 orders of magnitude confirm this simple picture, and a universal constant, a decay per unit length characteristic for many proteins, exists on this scale. The experimental data for the present Ru compounds show that on a finer scale of variation of only 2 orders of magnitude of k^{max} , there is only a very rough or perhaps no, in some cases, simple relation between distance and the coupling (or rate). For example, for His39 and His62 compounds, the distance between two metals is almost the same, yet the experimental rate changes by more than 2 orders of magnitude.

A qualitative explanation for this phenomenon was proposed in terms of atom-by-atom tunneling paths.¹⁷ According to this model, the effective electronic tunneling distance does not coincide with the actual geometrical distance between donor and acceptor. Although, in detail the picture of such atom-byatom tunneling paths along the network of chemical bonds and jumps through space between bonds of the protein matrix are an oversimplification, and for this reason may mainly be used for qualitative discussion, it does capture qualitatively the essential element that the concrete chemical structure of the protein matrix is important. A more realistic model the description using amino acid paths^{21,22} involves chemically distinct units of the protein. The electronic structure calculation for such atom-by-atom or amino acid-by-amino acid paths has confimed quantitatively that the protein matrix is a very inhomogeneous medium. A relatively small number of amino acids most important for electron transfer represent a reduced and useful model of a protein.21,22

The results of our calculations and a preliminary comparison with amino acid pathways, presented below, confirm that the reduced form of the protein provides a reasonable description of the most important part of the protein matrix, given the uncertainties and low quality of electronic structure calculations. The results also show that a qualitatively accurate description of the details of donor and acceptor wave functions in the calculation reveals that in addition to inhomogeneous factors governing the reaction rates, there is a stereochemical factor of mutual orientation of donor—acceptor orbitals. The latter effect adds more complexity to the general picture of variations of electron-transfer rates in proteins.

The donor and acceptor wave functions of the metal ions were constructed as described in the previous section, and the Hamiltonian matrix of the rest of the system was calculated with the extended Hückel basis set. The overlap matrix S_{ij} was calculated with a variational cutoff distance between pairs of atoms, and nondiagonal elements of the Hamiltonian were calculated with the standard use of the Wolfsberg—Helmholtz formula^{21,22,23}

$$V_{ii} = KS_{ii}(E_i + E_i)/2 (4.1)$$

where the E_i 's are orbital energies and the empirical parameter K equals $1.75.^{33}$ For the radial part of the s and p orbitals, a single-exponential—and for the d orbitals of metal atoms a double-exponential—representation was used with the same atomic parameters as in the standard extended Hückel calculations. By using charge-transfer spectra to determine the position of the metal orbitals relative to those of the ligands, no adjustable parameters were used in the calculation.

There are three relevant d orbitals for the electron donor and three for the acceptor. For each pair of donor—acceptor orbitals and for their combinations, the effective superexchange coupling element was calculated for several slightly different energies,

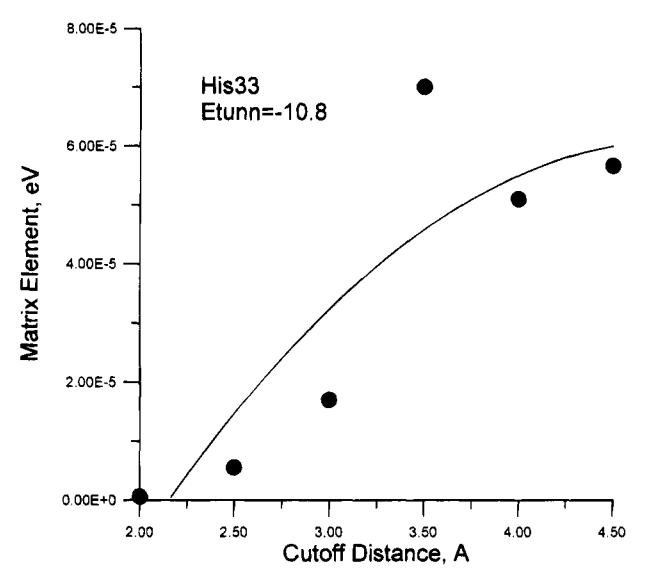


Figure 1. Cutoff distance dependence of the matrix element.

but in the range that corresponds to the charge-transfer spectra of ref 32, as discussed in the previous section. The typical splittings of the t_{2g} for Fe and Ru by the distorted octahedral geometry of the donor and acceptor complexes are shown in Table 1. The data are in general qualitative agreement with the conclusions of ref 32. However, there is a certain degree of uncertainty both in the Boltzmann factors for the Ru complex (discussed after eq 3.6) and in the geometry of the calculated structures. These uncertainties motivated us to calculate various possibilities of how the effective coupling could be formed between the three orbitals of the donor and three orbitals of the acceptor t_{2g} subshells.

In a first series of calculations, we explored how the direct long-distance interactions (distances longer than the typical bond lengths) between individual atomic orbitals of the protein matrix affect the net calculated tunneling probability. Typical data of this series are shown in Figure 1 where the cutoff distance for

direct atom—atom interaction was varied. If the cutoff distance is approximately the same as typical bond lengths, then only a network of transitions over chemical bonds in the protein is involved in the superexchange coupling. We find that the matrix elements for such calculations are several orders of magnitude smaller than the observed ones and that the coupling increases dramatically if the interaction distance is increased beyond the typical bond lengths. On the other hand, as is seen from Figure 1, the matrix element does not change substantially for cutoffs beyond 5 Å. The rather sharp transition to more or less saturated values shows that interaction distances between 2.5 and 3.5 Å provide critical links. These calculations confirm the conclusion that Beratan et al. reached earlier¹⁷ that "through space" transitions are important for electronic tunneling through protein media. These transitions serve as bottlenecks for the overall tunneling.

Although we observe saturation of the calculated values of the matrix element, there are, nevertheless, fluctuations of the calculated coupling as the cutoff distance changes in the range 3.5-5.0 Å. These fluctuations provide one source of estimate of the quality of the theoretical numbers.

The principal calculations were performed for several energies in the interval between -11.0 and -10.0 eV. This region corresponds to the experimental data of ref 32 on the charge-transfer spectra between porphyrin and Fe orbitals in the heme in a number of ferric cytochromes. This energy interval falls in the window in the spectral density of both the heme and the Ru complex calculated separately and shown in Figures 2 and 3. The energy gap between HOMO and LUMO in the heme is between -11.4 and -9.7 eV and for Ru complex between -11.9 and -9.7 eV. Our Hückel calculations performed on the d shells of metal ions with only nearest atomic ligands included in the calculations place the t_{2g} subshell in approximately the same energy interval, Table 1.

The principal calculated results are shown in Figures 4-9 for two tunneling energies, -10.75 and -11.0 eV, which seem to be in better agreement with the experimental data than for other energies. The experimental and calculated values are

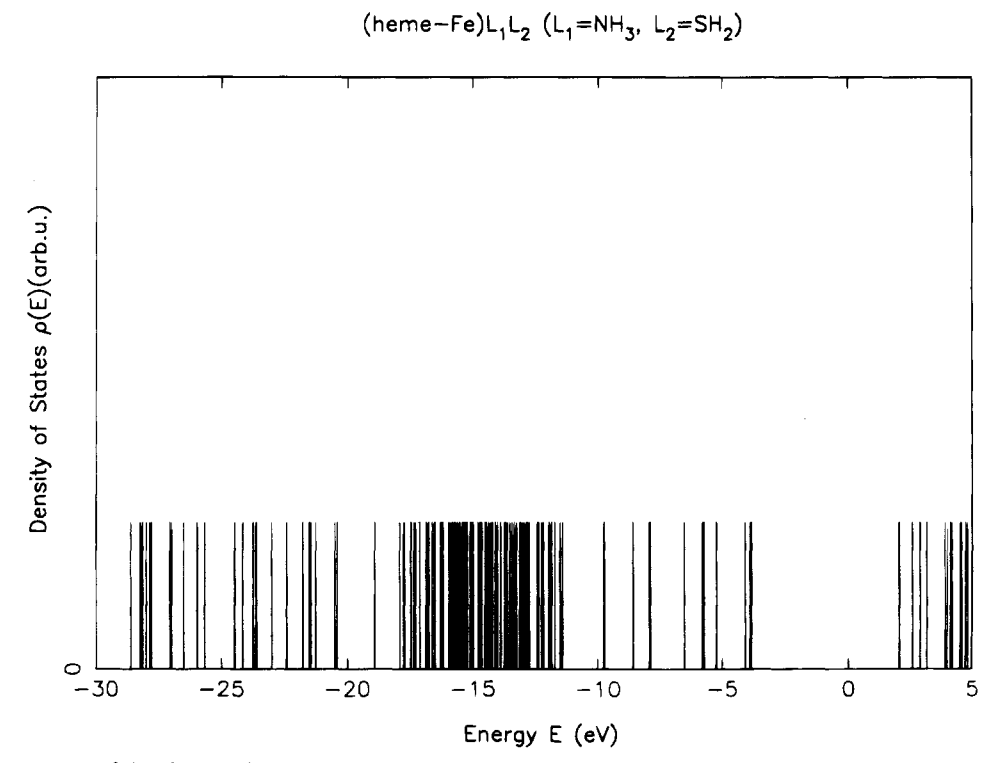


Figure 2. Energy spectrum of the electron donor complex.



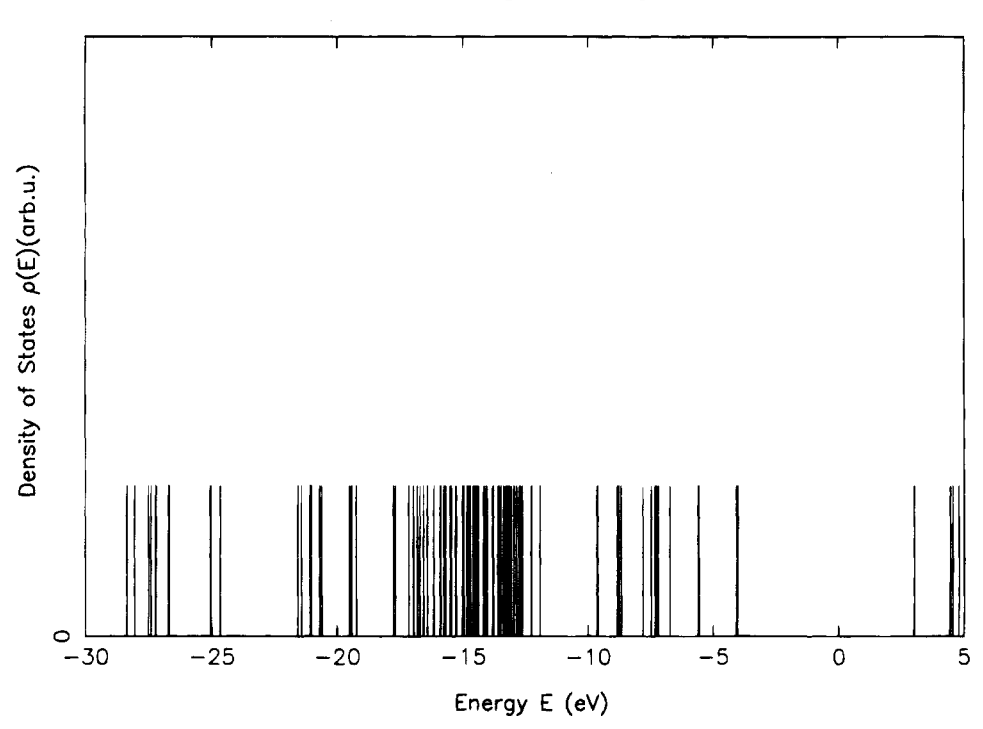


Figure 3. Energy spectrum of the electron acceptor complex.

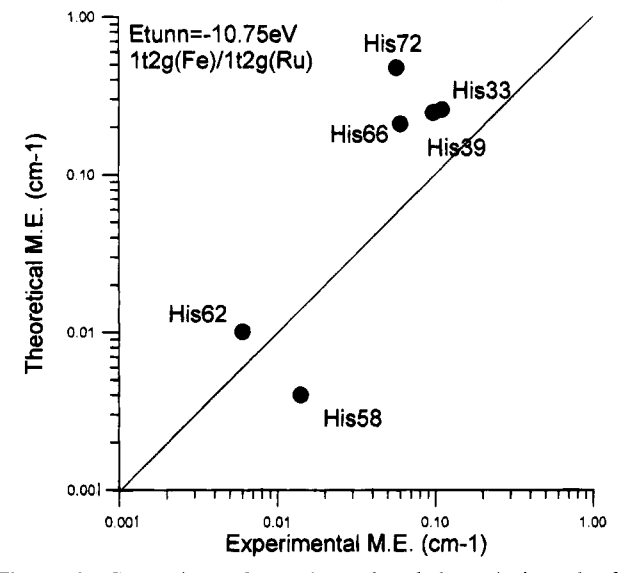


Figure 4. Comparison of experimental and theoretical results for tunneling energy of -10.75 eV. One level of the electron donor (Fe) and one level (upper) of the electron acceptor (Ru) are participating in the coupling.

shown in the same figures for comparison. In an ideal correlation between experimental and theoretical data, all points of Figures 4–8 would be located on a straight line with a slope of unity. Such an excellent agreement would probably be fortuitous, given the degree of uncertainty in both theoretical and experimental data. The general tendency, however, to have coupling much stronger for His39 than for His62, although the distance between donor and acceptor is approximately the same, seems to be a rather stable theoretical result. Obtaining a correlation with the small changes in matrix elements in His33 and -39 and in His66 and -72 is beyond the capabilities of the current theoretical methods. Our current estimates of the uncertainties involved, following from the scatter of theoretical

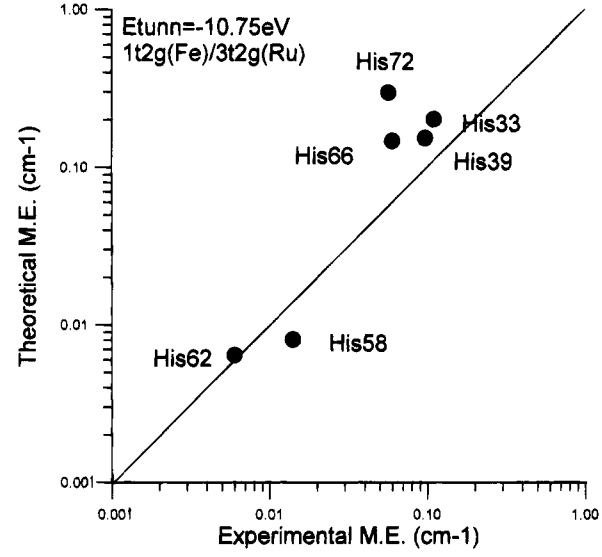


Figure 5. Same as in Figure 4 but with all three levels of the acceptor participating in the reaction.

data, show that even an accuracy within a factor of 2-3 is probably too much to expect from the present level of calculations.

For the His79 compound, only a lower limit for the experimental value of the rate constant (and matrix element) is known,⁸ $H_{\rm DA} > 0.6~{\rm cm}^{-1}$. This reaction is by far the fastest in the series. In our calculation, we observe the same qualitative picture, with our electronic coupling being an order of magnitude larger than the largest value for other compounds. Because the experimental value is not known exactly, we do not discuss further details of calculation for the His79 compound.

In Table 2, results are given for the coupling element between individual components of the t_{2g} shells of the metal ions. One particularly remarkable feature of the results shown in Table 2 is that the coupling for different components can vary by an order of magnitude for the same tunneling energy. The different

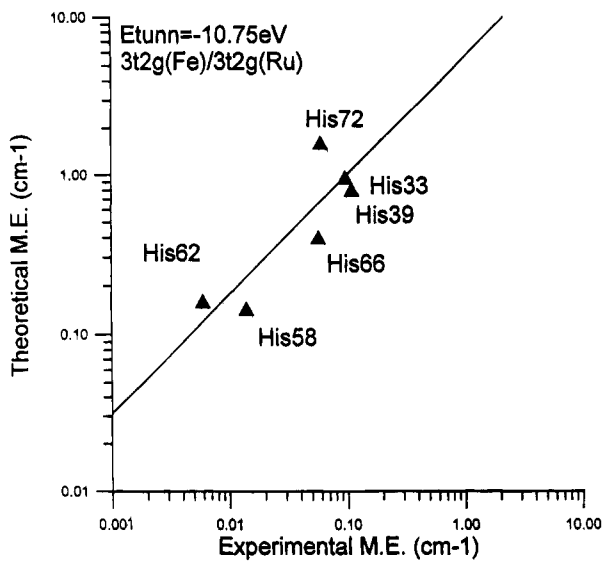


Figure 6. Same as in Figure 4 but with three donor orbitals and three acceptor orbitals participating in the reaction.

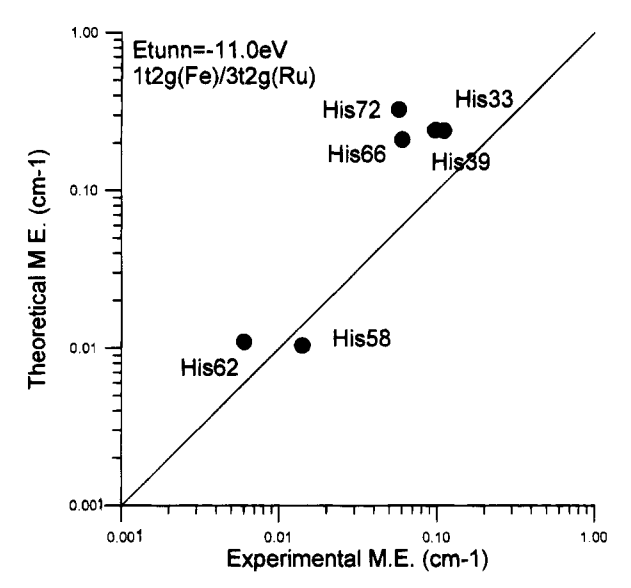


Figure 7. Same as in Figure 5 but for tunneling energy of -11.0 eV.

components of the t subshells, d_{xy} , d_{xz} , and d_{yz} , have different spatial orientation, and they are fixed in space with respect to the structure of the whole complex. Thus, in this situation, the electronic coupling depends strongly not only on the structure of the intervening medium but also on the relative orientation of the donor and acceptor complexes with respect to each other and with respect to the bridge, even when the initial and final electronic states are localized on the metal ions. This effect occurs because the electronic density of the donor and acceptor states is fixed by the position of the ligands coordinated to a metal ion. Such a strong stereochemical effect would be expected if the initial or the final state was delocalized orbitals of the whole complex with a strong degree of asymmetry, as for example in the heme, but it occurs also in the present case, where the ligands affect the orientation of an individual metal's atomic orbitals. Similar stereochemical effects were discussed recently in ref 40.

An important consequence of the specific nature of the donor and acceptor states, and in particular of the symmetry of t_{2g} orbitals, is that some paths connecting atoms of the donor and acceptor complexes will not participate in the coupling between donor and acceptor orbitals localized on the metal ions. All s orbitals of the ligands, for example, will be strongly decoupled

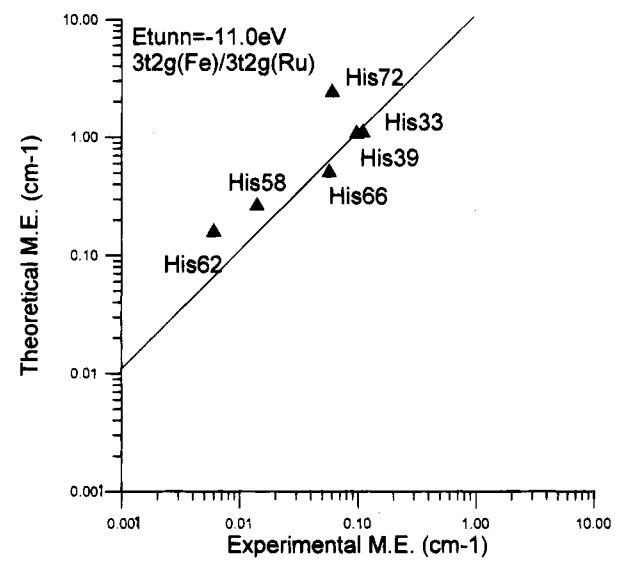


Figure 8. Same as in Figure 6 but for tunneling energy of -11.0 eV.

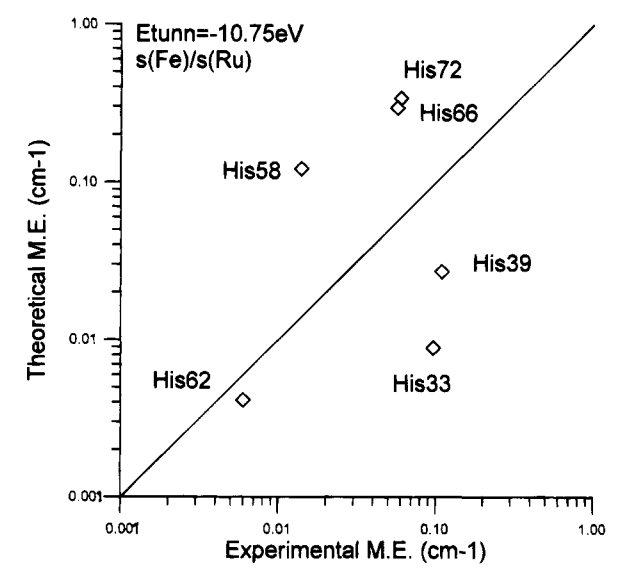


Figure 9. Comparison of experimental and theoretical data for electronic coupling of effective s orbital of donor and acceptor states. Tunneling energy is -10.75 eV.

from the donor/acceptor states for the systems discussed here and for systems with similar electronic structure. Thus, all σ paths which start on ligands and which involve as a first step a σ bond may not participate in a major way in the coupling. This feature has to be taken into consideration when the pathway model is applied.

The calculated results, including those shown in Figures 4–8, for two tunneling energies, -10.75 and -11.0 eV, are qualitatively similar. The difference in calculated matrix elements when only one (upper) level of the acceptor (Ru³⁺) is considered and the case when all three levels are involved in the reaction is not significant, as seen, for example, by comparing Figures 4 and 5. However, we find that there is a drastic difference in the results when one or all three final states of Fe³⁺ are involved in the reaction. This difference can be seen by comparing Figures 5 and 6 and comparing Figures 7 and 8. The difference in the results for the Ru and Fe ions could be attributed to a number of factors, one of which might be a larger distortion of the octahedral symmetry of the donor state.

In Figures 4-8, we have presented contributions of various levels of the donor and acceptor complexes to the total matrix element. As discussed earlier, the appropriate procedure for

TABLE 3: Comparison of All-Atom Model and a Reduced Model of a Protein Consisting of Only Most Important Amino Acids from refs 21 and 22^a

HisX, X	H _{DA} , exact	H_{DA} , AA paths	
39	0.20	0.24	
33	0.15	0.12	
66	0.14	0.56	
72	0.30	0.51	

^a Matrix elements were calculated for tunneling energy $E_{\text{tunn}} = -10.75 \text{ eV}$.

comparison of our results with experiment is to use all three levels of Fe (bacause of a small difference in their ΔG^0) and to weight the contribution of each of the Ru levels with the appropriate Boltzmann factors, as in eq 3.5. The results in Table 2 comparing the sum of three Ru levels with the d_{zx} Ru level indicate that the latter is usually the dominant contributor. If its Boltzmann factor is much less than the unity tacitly assumed in Figure 4 and than the $^{1}/_{3}$ assumed in Figures 5–8, then the calculated matrix element is overestimated in these figures, contributing thereby to the discrepancy between the absolute values of the calculated and experimental values of H_{DA} in Figures 6 and 8.

In Figure 9, the coupling calculated with effective s orbitals localized on metal ions is shown. In this case, mostly σ paths contribute to the coupling. The drastic difference in correlation with experimental data compared with the accurate treatment of the donor and acceptor wave function is a remarkable demonstration of the importance of symmetry and stereochemical effects in long-distance superexchange electronic coupling.

The present calculation, which includes all atoms of the system, allowed us to address the question of which part of the protein is most important for electronic coupling. In Table 3, the data for all-atom calculations and for the reduced model of four proteins with values of H_{DA} clustered in the range 0.05- $0.1~{\rm cm^{-1}}$ are shown. There is an approximate agreement with a factor of 2 or so. The reduced model is a small number of amino acids identified in refs 21 and 22 for several proteins. The amino acids so included correspond to "extended" amino acid paths defined by Siddarth and Marcus. The results are not strictly comparable since in the AI search used in refs 21 and 22, the axial ligands and resulting octahedral distortion were omitted. Further investigation using the search procedure will be done in our future work. The quality of the approximation of the reduced model varies for different proteins, but in some cases shown in Table 3, the agreement between exact calculations and the reduced form is quite reasonable, showing that is indeed possible to identify the reduced part of the protein which mainly provides the coupling between donor and acceptor in biological systems.

Acknowledgment. It is a pleasure to dedicate this paper to our friend Mostafa El-Sayed and to acknowledge his many contributions in physical chemistry. The financial support of the National Science Foundation and the Office of Naval Research is acknowledged. This research was also supported by a grant from the International Joint Research Program of NEDO (Japan). A.A.S. acknowledges with pleasure the start-up funds provided by the Chemistry Department at UC Davis and also many useful discussions with Dr. C. Winstead at Caltech of the computational aspect of the problem considered in the present paper. The access to computational resources of the JPL—Caltech Supercomputing Project is gratefully acknowledged.

Appendix

In this Appendix, the matrix form for the superexchange matrix element is derived for the case when the basis set used for matrix representation of the Hamiltonian operator is nonorthogonal, i.e., when the overlap matrix is not diagonal. This problem arises, for example, for the extended Hückel basis set considered in the present paper. We present a detailed derivation of the expression used in our calculations because a different expression has been published earlier in the literature.^{27,28}

Suppose we have a complete set of nonorthogonal basis functions, $|i\rangle$ (the extended Hückel basis in our case). The expansion of unity in such a basis is written as follows:

$$1 = \sum_{ij} |i\rangle S_{ij}^{-1} \langle j| \tag{A.1}$$

This relation is easy to verify by taking a matrix element of both sides of eq A.1 in the basis $|i\rangle$. Inserting this expansion on both sides of the resolvent operator in eq 2.2, we obtain

$$H_{\rm DA} = A_i^+ S_{ii}^{-1} \langle j | (E - H^B)^{-1} | k \rangle S_{kl}^{-1} D_l \qquad (A.2)$$

where the column vector D and the row vector A^+ are given by convention of omitting summation signs over repeated indices.

$$D_{l} = \langle l|V|D\rangle \tag{A.3}$$

$$A_i^+ = \langle A|V|i\rangle \tag{A.4}$$

The problem is now reduced to the calculation of the matrix of the resolvent operator in the middle of eq A.2. For the resolvent operator (Green's function), we have

$$G = (E - H^B)^{-1}$$
 $G(E - H^B) = 1$ (A.5)

Taking a matrix element of both sides of the last expression in the basis $|i\rangle$ and inserting the expansion of unity between G and $E - H^B$, eq A.1, we obtain the following relation:

$$G_{ij}S_{jk}^{-1}(ES_{kl} - H_{kl}^{B}) = S_{il}$$
 (A.6)

i.e., in matrix notation

$$GS^{-1}(ES - H^{B}) = S \tag{A.7}$$

Multiplying the last equation by S^{-1} on the left and by the inverse of the matrix $ES - H^B$ on the right, we obtain in the matrix form

$$S^{-1}GS^{-1} = (ES - H^{B})^{-1}$$
 (A.8)

Hence, eq A.2 can be written in the form

$$H_{\rm DA} = A_i^+ (ES - H)_{ij}^{-1} D_j$$
 (A.9)

The matrix in this equation is the inverse of $ES_{ij} - H_{ij}$, calculated in the nonorthogonal basis set, and vectors A and D are given by (A.3) and (A.4).

References and Notes

(1) (a) Devault, D. Quantum Mechanical Tunneling in Biological Systems; Cambridge University: Cambridge, 1984. (b) Electron and Proton Transfer in Chemistry and Biology; Miller, A., et al., Eds.; Elsevier: Amsterdam, 1992. (c) Long Range Electron Transfer in Biology; Springer: New York, 1991. (d) Metal Ions in Biological Systems; Sigel, H., Sigel, A., Eds.; Marcel Dekker: New York, 1991; Vol. 27. (e) "Electron Transfer." Chem. Rev. (Special Issue) 1992, 92.

(2) (a) Fox, M.; Jones, W., Jr.; Watkins, D. Chem. Eng. News 1993, March 15, 35–48. (b) Wasielewski, M. R. Chem. Rev. 1992, 92, 435. (c) Gust, D.; Moore, T. A. Science 1989, 244, 35. (c) Photoinduced Electron Transfer; Fox, M., Chanon, M. Eds.; Elsevier: Amsterdam, 1988. (d) Weber, S. Chem. Rev. 1990, 90, 1469.

- (3) (a) Molecular Electronics; Ashwell, G. J., Ed.; Research Studies: New York, 1992. (b) Molecular Electronics and Molecular Electronic Devices; Sienicki, K., Ed.; CRC: Boca Raton, FL, 1993.
 - (4) Deisenhofer, J.; Michel, H. Sciences 1989, 245, 1463.
 - (5) Winkler, J. R.; Gray, H. B. Chem. Rev. 1992, 92, 369.(6) Moser, C. C.; Keske, J. M.; Warncke, K.; Farid, R. S.; Datton, P.
- (6) Moser, C. C.; Keske, J. M.; Warncke, K.; Farid, R. S.; Datton, P. L. Nature 1992, 355, 796.
- (7) Casimiro, D. R.; Richards, J. H.; Winkler, J. R.; Gray, H. B. J. Phys. Chem. 1993, 97, 13073.
- (8) Wuttke, D. S.; Bjerrum, M. J.; Chang, I.; Winkler, J. R.; Gray, H. B. Biochim. Biophys. Acta 1991, 1101, 168.
- (9) Chang, İ.-Jy.; Gray, H. B.; Winkler, J. R. J. Am. Chem. Soc. 1991, 113, 7056.
- (10) Marcus, R. A.; Sutin, N. Biochem. Biophys. Acta 1985, 811, 265.
- (11) Ulstrup, J. Charge Transfer in Condensed Media; Springer: Berlin, 1979.
- (12) (a) Gehlen, J. N.; Marchi, M.; Chandler, D. Science 1994, 263, 499. (b) Marchi, M.; Gehlen, J. N.; Chandler, D.; Newton, M. J. Am. Chem. Soc. 1993, 115, 4178.
- (13) Parson, W.; Chu, Z.-T.; Warshel, A. Biochim. Biophys. Acta 1990, 251, 1017.
- (14) Treutlein, H.; Schulten, K.; Brunger, A. T.; Karplus, M.; Deisenhofer, J.; Michel, H. *Proc. Natl. Acad. Sci. U.S.A.* **1992**, 89, 75.
 - (15) Thompson, M.; Zerner, M. J. Am. Chem. Soc. 1991, 113, 8210.
 - (16) Newton, M. D. Chem. Rev. 1991, 91, 767.
- (17) Beratan, D. N.; Betts, J. N.; Onuchic, J. N. Science 1991, 252, 1285.
 - (18) Kuki, A.; Wolynes, P. G. Science 1987, 236, 1647.
 - (19) Larsson, S. J. Am. Chem. Soc. 1981, 103, 4034.
 - (20) Broo, A.; Larsson, S. Int. J. Quant. Chem. 1989, 16, 185.
- (21) Siddarth, P.; Marcus, R. A. J. Phys. Chem. 1993, 97, 2400; 1993, 97, 6111.
 - (22) Siddarth, P.; Marcus, R. A. J. Phys. Chem. 1992, 96, 3213.

- (23) Liang, C. X.; Newton, M. D. J. Phys. Chem. 1993, 97, 3199.
- (24) Evenson, J. W.; Karplus, M. J. Chem. Phys. 1992, 96, 5272.
- (25) Evenson, J. W.; Karplus, M. J. Science 1993, 262, 1247.
- (26) Gruschus, J. M.; Kuki, A. J. Phys. Chem. 1993, 97, 5581.
- (27) Regan, J. J.; Risser, S. M.; Beratan, D. N.; Onuchic, J. N. J. Phys. Chem. 1993, 97, 13083.
- (28) Risser, S.; Beratan, D. N.; Mead, T. J. Am. Chem. Soc. 1993, 115, 2508.
 - (29) Stuchebrukhov, A. A. Chem. Phys. Lett. 1994, 225, 55.
- (30) Ballhausen, C. Introduction to Ligand Field Theory; McGraw-Hill: New York, 1962.
- (31) Lever, A. B. P. Inorganic Electronic Spectroscopy; Elsevier: Amsterdam, 1984.
- (32) Gadsby, P. M. A.; Thomson, A. J. J. Am. Chem. Soc. 1990, 112, 5003.
- (33) Yates, K. Hückel Molecular Orbital Theory; Academic: New York, 1978.
- (34) Sparse Matrices. Reference Manual; Cray Research, Inc., 1993.
- (35) Tezduyar, T.; Aliabadi, S.; Behr, M.; Johnson, A. Computer 1993, 26, 27-36.
- (36) Golub, G. H.; Van Loan, C. F. *Matrix Computations*; Johns Hopkins University: Baltimore, 1989.
- (37) Press, W. H.; Flannery, B. P.; Teukolsky, S. A.; Vetterling, W. T. Numerical Recepes; Cambridge University: 1988.
- (38) BIOGRAF, Molecular Simulations, Inc. The program was originally written by S. L. Mayo, B. D. Olafson, and W. A. Goddard III.
- (39) If one integrated a semiclassical tunneling expression over an array of paths in 3D space from donor to acceptor, the result would have an approximate exponential dependence on the donor—acceptor separation.
- (40) Newton, M. In *Perspectives in Photosynthesis*; Jortner, J., Pullman, B., Eds.; Kluwer Academic: Amsterdam, 1989; p 157.

JP942571H